Photodissociation dynamics of lithium chloride: Contribution of interferometric predissociation

B. H. Hosseini,[1,2,a)] P. F. Weck,[3,b)] H. R. Sadeghpour,[1,c)] K. Kirby,[1,d)] and P. C. Stancil[4,e)]
[1]*ITAMP, Harvard-Smithsonian Center for Astrophysics, Cambridge, Massachusetts 02138, USA*
[2]*Fakultät Für Biophysikalische Chemie, Im Neuenheimer Feld 253, Universität Heidelberg, 69120 Heidelberg, Germany*
[3]*Harry Reid Center for Environmental Studies and Department of Chemistry, University of Nevada Las Vegas, Las Vegas, Nevada 89154, USA*
[4]*Department of Physics and Astronomy and Center for Simulational Physics, University of Georgia, Athens, Georgia 30602-2451, USA*

(Received 16 November 2008; accepted 23 December 2008; published online 5 February 2009)

Continuum photoabsorption of lithium chloride (LiCl) was investigated using a coupled-channel time-dependent wave packet approach. Photodissociation cross sections for the production of ground-state Li and Cl atoms were computed up to temperatures of 1500 K for a thermal distribution of rotational levels. At such temperatures, LiCl is believed to be the primary Li-bearing gas in cool stellar atmospheres. Narrow Rydberg resonances in the total absorption spectrum are found to dominate the thermally averaged cross section due to the large density of Rydberg states in the predissociation gap. Comparison with measured photoabsorption cross sections, where available, is made. © *2009 American Institute of Physics*. [DOI: 10.1063/1.3072094]

I. INTRODUCTION

Monatomic lithium has been detected in numerous stars, substellar-mass objects,[1] and in the interstellar medium.[2] Most of the lithium observed throughout the universe is believed to be primordial, i.e., formed during the era of Big Bang nucleosynthesis. Lithium is also formed in the galaxy through spallation reactions involving cosmic rays. However, once lithium finds itself in the core of a star it is destroyed via nuclear processes with protons. Therefore, understanding the abundance of Li has crucial implications for theories of the early universe, interstellar processes, and galactic and stellar evolution.[3] In low-temperature environments, a significant amount of Li can be sequestered into molecular species such as LiCl, LiH, and LiOH. Indeed, as shown by thermochemical equilibrium calculations of cool dwarf atmospheres,[4] LiCl is predicted to be the dominant Li-bearing gas for effective temperatures below 1500 K and low total pressure. However, LiCl line opacity calculations reveal that synthetic spectra predicted for young and old T dwarfs, with and without incorporating the LiCl line absorption, exhibit relative flux differences of less than 20%.[5]

The dominant LiCl opacity due to bound-bound transitions occurs in the mid-infrared where the fundamental vibration band is the strongest. On the other hand, molecular photodissociation due to electronic transitions could possibly provide some continuum opacity in the ultraviolet (UV) spectra of cool stars[6] or play a role in nonequilibrium chemistry. Quantifying the LiCl photodissociation cross section could also bring insights into the fact that LiCl was not detected in the cool molecular gas envelope, formed during the asymptotic giant branch phase, of the protoplanetary Egg Nebula, though NaCl and AlCl have been observed.[7] LiCl has also been searched for unsuccessfully in the Sagitarius B2 giant star-forming molecular cloud lying near the center of the galaxy[8] and in the circumstellar envelope of the super-Li-rich carbon star IY Hya. Mass loss from such objects can increase the Li abundance in the interstellar medium.[9]

Photodissociation of an alkali-halide molecule represents one of photochemistry's greatest triumphs due to its simplicity. It is a prototypical example of a nonadiabatic curve crossing system and of chemical reaction on femtosecond timescales.[10–12] For alkali-metal halides, the avoided crossing occurs when the Born–Oppenheimer (BO) electronic potential energy curves of the covalent lowest excited state, $B\ ^1\Sigma^+$, and the ionic ground state, $X\ ^1\Sigma^+$, become degenerate at an internuclear distance typically near $R \sim 10$ a.u. The avoided crossing arises because the two molecular states correlating to two neutral atoms and the ion pair (Li^+ and Cl^-) have the same symmetry ($^1\Sigma^+$). The energy gap between the ionic and covalent channels is about 2 eV in the separated atom or dissociation limit. The strong Landau–Zener coupling between the two Σ^+ states and the ionic nature of the electronic ground state dictate that highly excited rovibrational levels in the ionic channel, lying in the dissociation gap (Fig. 1), and the covalent continuum interact.

In this work, we employ recent *ab initio* BO potential energies and permanent and transition dipole moment functions of LiCl (Ref. 13) in a coupled-channel time-dependent quantum mechanical calculation[10] to obtain predissociation dynamics and photodissociation cross sections. We follow the prescription in Ref. 14 for obtaining the diabatic potential matrix and calculate partial continuum photoabsorption spec-

[a)]Electronic mail: hadji-hosseini@stud.uni-heidelberg.de.
[b)]Electronic mail: weckp@unlv.nevada.edu.
[c)]Electronic mail: hrs@cfa.harvard.edu.
[d)]Electronic mail: kirby@cfa.harvard.edu.
[e)]Electronic mail: stancil@physast.uga.edu.

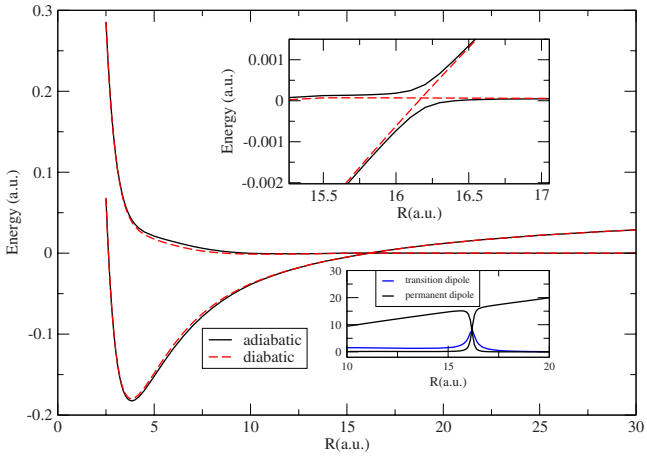

FIG. 1. (Color online) The adiabatic and diabatic potential curves of LiCl $X\ ^1\Sigma^+$ and $B\ ^1\Sigma^+$ states, and in the bottom inset, the X dipole moment, the B dipole moment, and the $B \leftarrow X$ transition moment.

tra at UV wavelengths for temperatures up to $T=1500$ K, typical of L dwarfs. A time-independent method is used to further confirm our results for the photodissociation cross sections for photon energies above the ion-pair dissociation limit. Atomic units (a.u.) are used throughout unless otherwise noted.

II. THEORETICAL FRAMEWORK

A. Fano formalism

The simple picture of rovibrational predissociation in alkali-halide molecules, in which a repulsive BO electronic potential energy curve crosses an attractive electronic energy curve, supporting discrete series of rovibrational levels, can be intuitively framed in the Fano configuration interaction formalism.[15] In the Fano picture, the excitation spectrum can be represented in a compact form

$$I(\omega) = I_0 \frac{(q+\epsilon)^2}{1+\epsilon^2}, \tag{1}$$

where I_0 is some frequency-independent background intensity, ϵ is a reduced dimensionless energy, which vanishes at the position of the resonance, and $-\infty \leq q \leq \infty$ is a measure of the lineshape asymmetry. When the lineshape drops into (rises from) the $\epsilon \leq 0$ side of the resonance, $q \geq 0$ ($q \leq 0$). For $q \to \infty$, the lineshape is inverted as a symmetric dip (window resonance or antiresonance). This expression for the line profile encapsulates many of the complicated coherent quantum interferences, resulting from the interaction of dissociating quantum pathways, in a single parameter, q. The highly asymmetric Fano resonances that result, attest to the coherent quantum interference that precedes the full dissociation in alkali halides. In our example, the vibrational predissociating Fano resonances are driven by the strong Coulomb interaction manifested in the ionic bond ($Li^+ - Cl^-$). The attractive Coulomb potential between the ion pairs leads to the emergence of an infinite vibrational spectrum, whose level spacing is governed by the Rydberg equation $E_v = -R_\infty/(v - \pi\mu_v)^2$, where R_∞ is the Rydberg constant and μ_v is some quantum defect for the vibrational series in the potential with quantum number v.

B. Electronic potentials

The adiabatic potential energy curves for the two lowest-lying $^1\Sigma^+$ electronic states of LiCl, $X\ ^1\Sigma^+$ and $B\ ^1\Sigma^+$, which correlate to the $Li(^2S)+Cl(^2P)$ neutral and $Li^+(^1S)+Cl^-(^1S)$ ion pairs, respectively, are shown in Fig. 1. For large values of R, the *ab initio* data of Weck *et al.*[13] were fitted to an attractive Coulomb potential augmented with a polarization term for the ionic channel and a decaying exponential potential for the covalent channel. The asymptotic splitting between the two curves is 1.74 eV, which is the difference in the ionization potential of Li (5.392 eV) and the electron affinity of Cl (3.653 eV). The adiabatic potentials were transformed to a diabatic representation, in which the molecular curves actually cross and the diabatic coupling is a smooth function of R. This diabatic representation is obtained in the basis which diagonalizes the adiabatic dipole operator

$$\mathbf{D}^d = \mathbf{C}^\dagger \mathbf{D}^a \mathbf{C}, \tag{2}$$

where $\mathbf{D}^{a,d}$, shown in Fig. 1 (inset), are, respectively, the dipole operators in the adiabatic and diabatic representations and $\mathbf{C}$ is the unitary transformation matrix.[14] The avoided crossing region near $R \sim 16.2$ a.u. is highlighted in Fig. 1 (inset) and the resulting diabatic curves which actually cross are also shown.

C. Wavepacket propagation

The Schrödinger equation in the diabatic representation for the two-channel problem is given by

$$i\hbar \frac{\partial \mathbf{\Psi}(R,t)}{\partial t} = \mathbf{H}^d \mathbf{\Psi}(R,t) = \left[-\frac{\hbar^2}{2\mu} \mathbf{I} \frac{d^2}{dR^2} + \mathbf{V}^d \right] \mathbf{\Psi}(R,t), \tag{3}$$

where $\mu = 10\,651.34$ a.u. is the reduced mass of the LiCl molecule, $\mathbf{I}$ is the 2×2 unity matrix, and $\mathbf{\Psi}$ is a two-component vector, each component representing the nuclear wave function on each electronic potential energy curve. In the diabatic representation, the potential matrix $\mathbf{V}^d$ is nondiagonal with the off-diagonal term resulting from the nonadiabatic coupling in the adiabatic representation.

The split-operator method,[16] which was used to solve the Schrödinger equation, employs a symmetric splitting of the kinetic and potential energy operators

$$\mathbf{\Psi}(t+\Delta t) = e^{-i\Delta t \mathbf{V}/2\hbar} e^{-i\Delta t \mathbf{T}/\hbar} e^{-i\Delta t \mathbf{V}/2\hbar} \mathbf{\Psi}(t) + O(\Delta t^3). \tag{4}$$

The action of the potential energy operator is carried out in coordinate space and that of the kinetic energy operator $\mathbf{T}$ in momentum space where it is diagonal. The fast-Fourier-transform algorithm is used to efficiently switch between the coordinate and momentum spaces following the application of each exponential operator. The wave packet propagation was performed with a number of different time slices and we chose a time grid size of 0.121 fs. A complex absorbing potential was placed at an internuclear distance, R, larger than that at which the flux was calculated to attenuate the

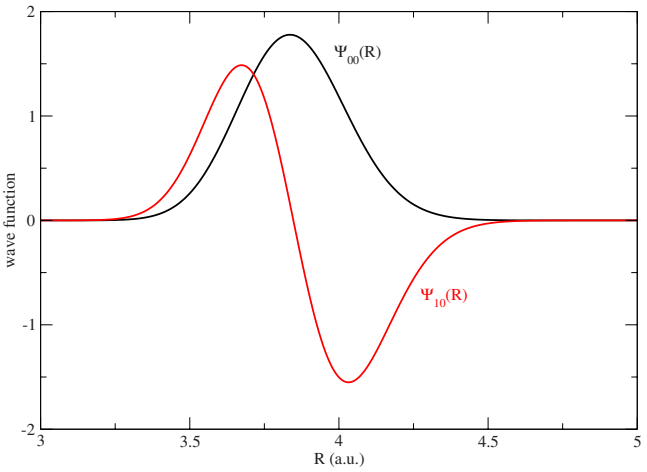

FIG. 2. (Color online) Ground vibrational and first excited vibrational wave functions in the ionic potential, illustrating the FC reflection principle.

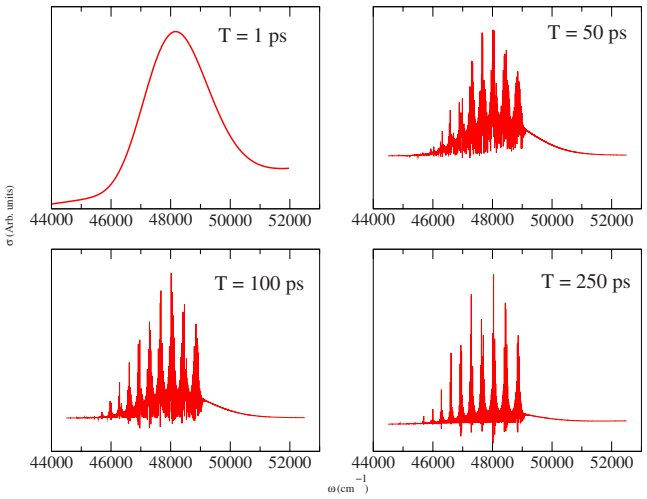

FIG. 3. (Color online) Temporal snapshots of LiCl photodissociation cross section. At short times (top left panel), only direct FC excitation is observed, followed later by the appearance of Rydberg vibrational progression (top right panel). Only at much later times, corresponding to many vibrational periods (lower panels), the periodic modulation in the photodissociation spectrum emerges.

dissociating part of the wave function and prevent artificial reflection back to the inner region. For the spatial representation of the wave function, we used an equally spaced grid of 3072 points in the region of $3 \leq R \leq 100$ a.u.

The partial predissociating cross sections were calculated by taking the Fourier transform of the autocorrelation function, $C(t)=\langle \mathbf{\Psi}(R,t=0) | \mathbf{\Psi}(R,t) \rangle$,[17] as

$$\sigma(\omega) = \frac{2\pi\omega}{3\hbar c} \int_{-\tau}^{\tau} dt w(t) C(t) e^{iEt/\hbar}, \tag{5}$$

where ω is the photon frequency, $\hbar$ and c are the reduced Planck constant and speed of light, and the energy is $E_{v''j''} + \hbar\omega$, with $E_{v''j''}$ the rovibrational energy of the initial state and $w(t)$ is a window function which vanishes at the limits of the time integral, τ.

Partial rotational cross sections for the $R(j)$ and $P(j)$ branches were calculated as

$$\sigma_j^+ = \sigma(j \rightarrow j+1) \quad \text{and} \quad \sigma_j^- = \sigma(j \rightarrow j-1), \tag{6}$$

up to $j_{\max}=39$, keeping the molecule in its ground vibrational level $(v=0)$—the upper bound is determined by the thermal excitation of rotational levels. The partial cross sections were added with statistical weights to give the photodissociation spectrum for a given j level,

$$\sigma_j = (j+1)\sigma_j^+ + j\sigma_j^-. \tag{7}$$

To calculate the cross section $\bar{\sigma}$ for a thermalized population of initial rovibrational states corresponding to a gas temperature T, we sum over the partial cross sections weighted by the level populations,

$$\bar{\sigma}(T) = \sum_{j=0}^{j_{\max}} p_j(T)\sigma_j, \tag{8}$$

where the population $p_j(T)$ corresponds to a Maxwell–Boltzmann distribution. We note that the first vibrational excited level $(v=1)$ has a node precisely where the ground vibrational level has a maximum, as shown in Fig. 2. In Refs. 10 and 18, it has been established that the broad photoabsorption feature in the spectrum occurs nearly instantaneously over 10–20 fs or a small fraction of vibrational period, thus resulting in a Franck–Condon (FC) reflection spectrum. It is also known that the FC factor is proportional to the square of the initial state wave function[19] at the Condon point. Therefore, we would expect the excited vibrational states to contribute little to the photodissociation spectrum, even if they were populated.

III. SPECTRAL RESULTS

Because the wave functions were obtained on a time grid, all frequency components are present in the final wave packet. It is therefore possible for different frequency scales to be sampled by taking slices in the time propagation. As an illustrative example and to demonstrate the complex structures that form in the spectrum as a function of time, we display in four panels in Fig. 3 the cross sections at 1, 50, 100, and 250 ps. Initially, the spectrum has a near-Gaussian shape, representing the vertical FC transition from the initial

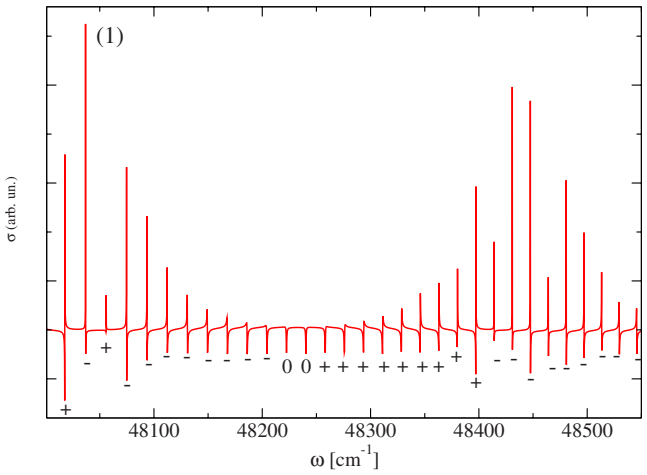

FIG. 4. (Color online) Double reversal of Fano asymmetry parameter. The periodic modulation of the photodissociation spectrum is also visible.

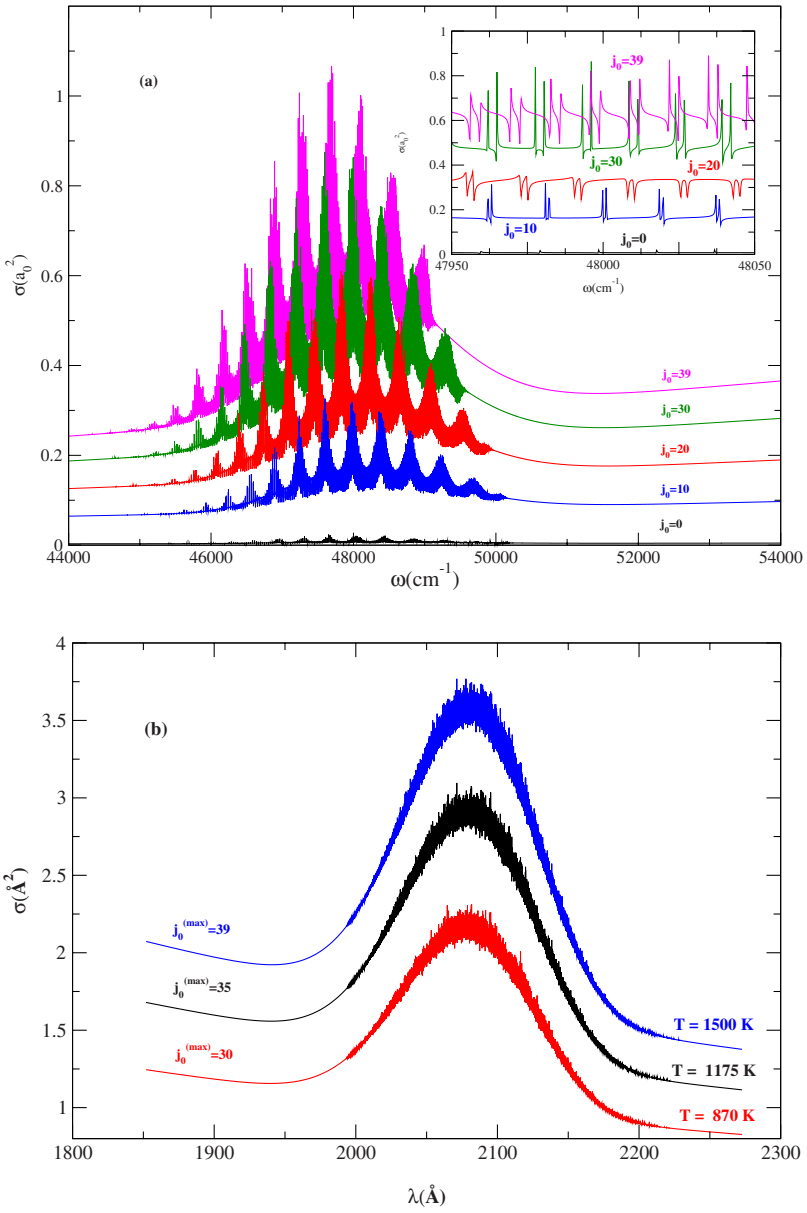

FIG. 5. (Color online) The summed partial cross sections at different slices for each value of the initial rotational level j_0 in (a). The inset in (a) amplifies the resonance structure near the FC region. The color code for each curve is the same as for the main curve in (a). In (b), the thermally averaged cross sections as a function of the wavelength are shown for temperatures up to $T=1500$ K.

$v=0$ rovibrational state. After a few picoseconds, the Rydberg rovibrational photodissociation is superimposed upon the Gaussian hump, and at later times, a periodic superstructure modulation forms atop the rovibrational structure. This has been shown to be due to an interferometric process in which different pathways to dissociation interact.[14] One noticeable feature is the abrupt cutoff of the high-frequency end of the spectrum that is due to the position of the absorbing potential; we have experimented with several grid scenarios and placement of the absorbing potential to obtain converged results.

Figure 4 shows an expanded view of the asymmetric Fano profiles for the interferometric resonances.[15] The sign of the Fano asymmetry parameter, q, is indicated in the figure, illustrating the periodic double reversal of the sign of q, itself a manifestation of the quantum interference effect in LiCl photodissociation. The periodic superstructure is also visible at the double reversal of the Fano parameter. In Fig. 5(a), the partial cross sections, summed up to the level j_0, where j_0 is an initial rotational level, are presented. The aim here is to show the behavior and magnitude of the predissociating resonances and the "piling up" effect on the total cross section. At a value of $j_0=39$, the results are converged for $T=1500$ K. The narrow Rydberg resonances dominate the total absorption spectrum and make a significant contribution to the thermally averaged cross section due to the large density of Rydberg states in the predissociation gap. We have confirmed that a single-channel time independent calculation of the photodissociation cross section above the ion-pair threshold is consistent with the time-dependent high-frequency results in Fig. 5(a).

The thermally averaged cross section as a function of wavelength in the UV is shown in Fig. 5(b), up to $T=1500$ K. The thresholds for photodissociation from the $v=0$, $j=0$ level occur at 2485 and 1842 Å for the covalent and ionic limits, respectively. The magnitude of the cross section is comparable to the low-resolution absorption cross section measured by Davidovits and Brodhead[20] though the experimental peak is shifted to ~2350 Å. However, a high concentration of dimers, possibly exceeding 60%, in the experi-

ment and our neglect of the 882 cm^{-1} fine-structure splitting of Cl may explain the discrepancy. We note that the magnitude of the LiCl cross section at the peak is ~1000 times larger than that of the $X \leftarrow B$ transition of MgH,[21] which peaks near 2800 Å. Since Mg begins to condense into refractory silicates like Mg_2SiO_4 and $MgSiO_3$ for atmospheric temperatures between 1700 and 1900 K in cool L dwarfs,[22] while Li is primarily in LiCl, the relative abundances of LiCl and MgH are likely comparable. Since LiCl does not condense into $LiAlO_2$ until the temperature falls below ~700 K,[22] it might be a significant UV opacity source, larger than that of MgH. In warmer L dwarfs or in cool dwarfs irradiated by a hotter and nearby companion, photodissociation may result in nonequilibrium effects in the chemistry of LiCl.

IV. CONCLUSION

Using a coupled-channel time-dependent wave packet method, we have investigated the photodissociation dynamics of LiCl below the ionic channel dissociation threshold. Cross sections for a thermal population of rotational levels have been computed and are compared with an early absorption measurement. LiCl has become of interest recently in connection with its possible presence in the atmospheres of cool brown dwarfs, spectroscopically classified as L dwarfs. Given the large cross section, photodissociation may play a role in the nonequilibrium photochemistry of LiCl in such objects.

ACKNOWLEDGMENTS

B.H.H. was supported by a grant from the Smithsonian Scholarly Studies Program. P.F.W. acknowledges support from NASA (NASA EPSCoR 2008 Proposal Development Award). H.R.S. and K.K. acknowledge support from a NSF grant to ITAMP at Harvard University and Smithsonian Astrophysical Observatory. P.C.S. acknowledges support from NASA Grant No. NNG04GM59G.

[1] J. D. Kirkpatrick, I. N. Reid, J. Liebert, R. M. Cutri, B. Nelson, C. A. Beichman, C. C. Dahn, D. G. Monet, J. E. Gizis, and M. F. Skrutskie, Astrophys. J. **519**, 802 (1999).
[2] D. C. Knauth, S. R. Federman, D. L. Lambert, and P. Crane, Nature (London) **405**, 656 (2000).
[3] A. J. Korn, F. Grundahl, O. Richard, P. S. Barklem, L. Mashonkina, R. Collet, N. Piskunov, and B. Gustafsson, Nature (London) **442**, 657 (2006).
[4] K. Lodders, Astrophys. J. **519**, 793 (1999).
[5] P. F. Weck, A. Schweitzer, K. Kirby, P. H. Hauschildt, and P. C. Stancil, Astrophys. J. **613**, 567 (2004).
[6] C. I. Short and J. B. Lester, Astrophys. J. **469**, 898 (1996).
[7] J. L. Highberger, K. J. Thompson, P. A. Young, D. Arnett, and L. M. Ziurys, Astrophys. J. **593**, 393 (2003).
[8] B. E. Turner, Astrophys. J., Suppl. Ser. **70**, 539 (1989).
[9] D. A. Lubowich, Nucl. Phys. A. **621**, 14 (1997).
[10] A. B. Alekseyev, H.-P. Lieberman, R. J. Buenker, N. Balakrishnan, H. R. Sadeghpour, S. T. Cornett, and M. J. Cavagnero, J. Chem. Phys. **113**, 1514 (2000).
[11] T. S. Rose, M. J. Rosker, and A. H. Zewail, J. Chem. Phys. **88**, 6672 (1988).
[12] A. H. Zewail, J. Phys. Chem. **100**, 12701 (1996).
[13] P. F. Weck, K. Kirby, and P. C. Stancil, J. Chem. Phys. **120**, 4216 (2004).
[14] S. T. Cornett, H. R. Sadeghpour, and M. J. Cavagnero, Phys. Rev. Lett. **82**, 2488 (1999).
[15] U. Fano, Phys. Rev. **124**, 1866 (1961).
[16] M. D. Feit, J. A. Fleck, and A. Steiger, J. Comput. Phys. **47**, 412 (1982).
[17] E. J. Heller, Acc. Chem. Res. **14**, 368 (1981).
[18] N. Balakrishnan, B. D. Esry, H. R. Sadeghpour, S. T. Cornett, and M. J. Cavagnero, Phys. Rev. A **60**, 1407 (1999).
[19] C. Boisseau, E. Audouard, J. Vigue, and P. S. Julienne, Phys. Rev. A **62**, 052705 (2000).
[20] P. Davidovits and D. C. Brodhead, J. Chem. Phys. **46**, 2968 (1967).
[21] P. F. Weck, P. C. Stancil, and K. Kirby, Astrophys. J. **582**, 1263 (2003).
[22] A. Burrows and C. M. Sharp, Astrophys. J. **512**, 843 (1999).